

Grid Connected Photovoltaic Power Plant Systems through Single Stage Inverter under Grid Faults

M.Shekar

**M.Tech Electrical Power Systems (EPS),
Department of EEE,
St. Martins Engineering College,
Hyderabad, Telangana, India.**

Mr.V.Sunil Kumar, ME

**Associate Professor,
Department of EEE,
St. Martins Engineering College,
Hyderabad, Telangana, India.**

Abstract:

In this paper the control of a single-stage grid-connected photovoltaic power plant (GCPPP) is developed to address the issue of inverter disconnection under various grid faults. There are three main reasons for inverter disconnection which are (i) excessive dc link voltage, (ii) excessive ac currents and (iii) loss of grid-voltage synchronization. The control of the inverter incorporates reactive power support in the case of voltage sags based on grid code requirements to ride-through the faults and support the grid voltages. Accordingly, another requirement of the grid codes is to control the reactive current injection under unbalanced voltage sags so that the voltages in the non-faulty phases do not exceed the specified limitations. All these issues are discussed in this paper for a case study of 1-MVA GCPPP using MATLAB/Simulink. The results illustrate the capability of the developed GCPPP to ride through different types of faults occurred on the grid side.

Index Terms:

Photovoltaic systems, Large-scale systems, Power system faults, Fault-ride-through, Reactive power support, battery energy storage system(BESS).

I.INTRODUCTION:

Nowadays, grid-connected photovoltaic power plants (GCPPPs) have received a great importance and popularity in both domestic and large-scale power generation. As the number and size of the photovoltaic (PV) power plants increase, new issues arise from both the PV power plant and grid sides. Some of these issues have been pointed out in Therefore, more investigations are required to understand the impact of

GCPPPs on existing power grids and to achieve stable and secure operation. Fault studies of GCPPPs have been widely reported in the technical literature. For instance, fault current contributions of PV power plants have been studied in Other research has focused on low-voltage ride through (LVRT) capability Techniques. For unbalanced voltage sags, a method to mitigate the peak output currents of a 4.5-kVA PV power plant in non-faulty phases is introduced in Another study in presents a proportional-resonant (PR) current controller for the current limiter to assure a sinusoidal output current without over current. However, in the mentioned methods, reactive power support has not been considered. For the grid-connected current source inverter-based PV power plants some studies have been reported in by considering symmetrical and asymmetrical types of faults and their impacts on the output current. However, the output current remains limited in all types of faults due to the implementation of a current source model for the inverter. For the dc side of the inverter, a study has been reported in which shows the impact of various types of faults on the voltage and current of the PV array. In, some research has been done on a superconducting magnetic energy storage (SMES) system that is used to store energy and regulate the ac currents and the dc-link voltage during voltage sags. In, a method has been introduced to control the positive and negative sequences besides limiting the output current not to exceed a predefined boundary. Considering a single-stage grid-connected inverter, no paper has proposed a comprehensive strategy for protecting both the dc and the ac sides of the inverter during unbalanced grid faults seems to be no paper that has discussed how the inverter has to be

designed and modified to accommodate various types of faults and address the fault-ride-through (FRT) capability based on the grid codes. The objective of this paper is to introduce some control strategies for single-stage GCPPPs that allow the inverter to remain connected under various types of grid faults based on the grid codes. PV inverter disconnection under grid faults is due to three main factors: (i) excessive dc-link voltage, (ii) excessive ac currents and (iii) loss of grid voltage synchronization, which may conflict with FRT capability. Moreover, during unbalanced conditions, the voltage in non-faulty phases should not exceed the specified limits due to reactive power injection. This paper is organized as follows. A summary of the grid codes (GCs) for medium voltage GCPPPs is presented in Section II. A case study for single-stage VSI based GCPPPs is introduced in Section III. The same section includes discussions on the implemented grid synchronization method as well as the control strategy to avoid excessive ac currents and excessive dc voltage under voltage sags is presented in Section IV. Grid faults. Classification of grid faults is presented in Section V. battery energy storage system (BESS) is presented in section VI. Design and analysis of single stage conversion with battery conversion is presented in section VII. MATLAB / SIMULATION RESULTS is presented in section VIII. Future scope is presented respectively. Finally, Section IX summarizes the conclusions.

II. GRID CODES REQUIREMENTS:

When connecting PV plants to medium voltage grids, it is necessary to provide them with dynamic support for the grid voltages. This dynamic support is referred to FRT technique in which the PV plant should stay connected in the case of grid faults depending on the fault time duration. They have also to provide support to the grid voltages by injecting reactive power. Considering the FRT capability, there are four major reasons for inverter disconnection during grid faults, which are the following ones: (1) excessive dc-link voltage, (ii) over current at the ac side and (iii) loss of grid voltage synchronization. Moreover, in the case of asymmetrical faults, (iv) the reactive current injected

must not exceed values that cause voltages to increase above 110% of the nominal value in the non-faulty phases.

II.1 GRID CODES:

As the German GCs are the most comprehensive codes for the different power levels of PV installations and integration technologies, this paper follows these codes as a basis for the discussions. During voltage sags, the GCPPP should support the grid voltage by injecting reactive current. The amount of reactive current is determined based on the droop control defined as follows.

$$i_{qref} = \text{droop} |de_L| I_n'$$

$$\text{for } \frac{|de_L|}{E_n} \geq 10\% \text{ and } \text{droop} \geq 2$$

Where droop is a constant value, deL is the amount of voltage drop, and I_n is the rated current of the PV inverter in dq coordinates, i.e., $I_n = \sqrt{3}I_n$, where I_n is the rated rms line current of the inverter. The amount of voltage drop deL is obtained based on the lowest rms value of the line-to-line voltages of the three phases at the terminal of the GCPPP, i.e., $e_{L \min}$ shown in Fig. 1. The rms voltage is obtained using the following expression:

$$e_{Lrms} = \sqrt{\frac{1}{T_w} \int_{t-T_w}^t e_L^2 dt}, \text{ with } T_w = \frac{T}{2}$$

Where L is the instantaneous line-to-line voltage, T_w is the window width for the rms value calculation, and T is the grid voltage period, which is equal to 20 ms for a grid frequency of 50 Hz. The resulting control diagram for the reactive current generation is depicted.

III. CASE STUDY FOR A SINGLE STAGE CONVERSION:

In this section, a 1-MVA single stage GCPPP is considered. It is modeled using MATLAB/SIMULINK and the system main

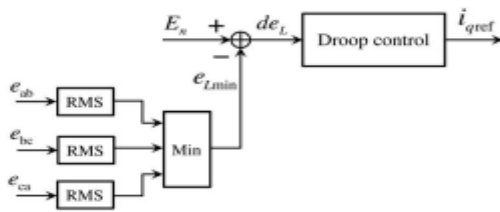


Fig 1. Droop control diagram for the reactive current reference provision.

specifications are summarized in Table I from the data given in 1. Fig. 2 shows the model of the GCPPP. In, concerning the FRT capability, the inverter disconnection factors are illustrated according to the GCs.

PV module specifications		PV inverter specifications	
Maximum operating voltage (V_{mpp})	35.6 V	Maximum dc power	1133 kW
Maximum operating current (I_{mpp})	8.29 A	Maximum dc input voltage	1000 V
Open circuit voltage (V_{oc})	44.3 V	Rated dc voltage	800 V
Short circuit current (I_{sc})	8.74 A	Apparent power rating (at STC)	1100 kVA
Number of parallel modules, n_p	155	Filter	$R = 1 \text{ m}\Omega$ $L = 150 \mu\text{H}$
Number of series modules, n_s	22	Transformer	1.2 MVA 20/0.415 kV Dyn11 50 Hz

Table.1 Case Study of Single Stage GCPPP System Specifications.

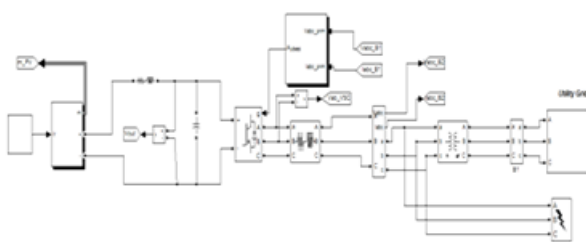


Fig 2. Simulation Diagram of a single-stage GCPPP

A. Grid voltage synchronization:

In grid-connected inverters, one important issue is the voltage phase angle detection. This is usually performed by phase locked-loop (PLL) technique based on a synchronous reference frame PLL (SRF-PLL), known as conventional PLL. The conventional PLL configuration does not perform well under unbalanced voltage sags and consequently may lead to

the inverter being disconnected from the grid. Several methods were proposed to extract the voltage phases accurately under unbalanced voltage conditions. In this paper, the method based on moving average filters (MAFs) introduced is applied, which was also used in] showing very satisfactory performance. In this method, the positive sequence of the voltage is extracted from the grid by means of an ideal low-pass filter. Then, the angle of the positive sequence is detected.

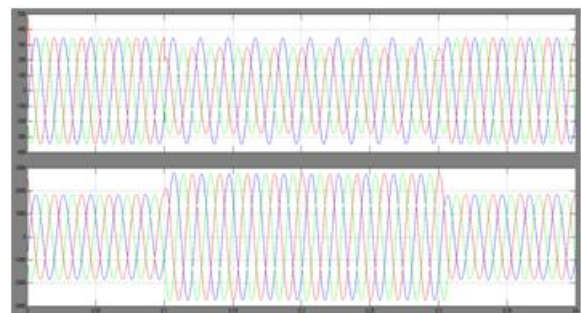


Fig 3. (a) Grid voltages and (b) grid currents at the LV side under 60% SLG voltage sag produced at MV side of the transformer.

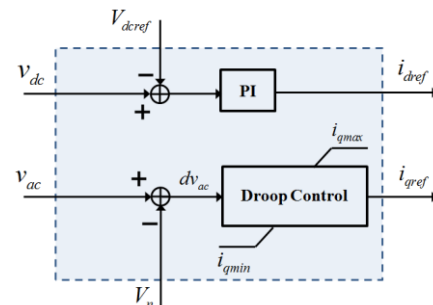


Fig 4. Basic schematic of the transformed dq reference currents.

B. Excessive AC Current:

Commercial grid-connected inverters have a maximum ac current value specified. If any of the currents exceed such value, the inverter is disconnected from the grid. Under a grid voltage sag, the d-component of the current (in the SRF) increases because the controller wants to maintain the active power injected into the grid and grid voltages are temporarily reduced. In addition to the increase of the d current component, the inverter has to inject reactive current during the fault to meet the FRT requirements.

The amount of reactive current is assigned according to the droop control given in (1). Since the d and q current components increase, this may lead the over-current protection to disconnect the inverter from the grid. In this case study, according to the specifications of the PV modules and their numbers of being connected in series and parallel given in Table I, the maximum power injected under standard test conditions (STC) is 1.006 MW. This power gives a rated rms current value of 1399.5 A (a peak value of 1979 A) at the low-voltage (LV) side of the transformer considering 100% efficiency for the GCPPP. According to the inverter datasheets, the maximum acceptable output current at the LV side of the transformer is 1532 A (a peak value of 2167 A). In the case of a fault, e.g., a single-line-to-ground (SLG) voltage sag at the MV side of the transformer as the one presented in Fig. 3, the output currents exceed the limits. This will lead to inverter disconnection, although it is not applied in this simulation. Unbalanced and distorted currents are produced because the instantaneous output power and the dc-link voltage have low-frequency ripples, and therefore, the active current reference contains low-frequency ripples as well. The final reference for the d current component (i_{dref}) should be limited considering the need of reactive current injection as shown in Fig. 4.

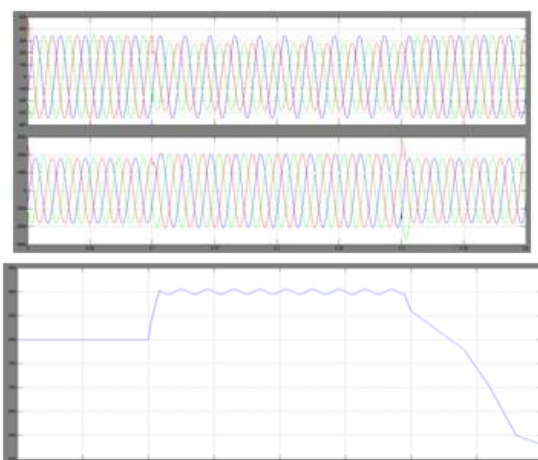


Fig 5. Adding the current limiter to the VSI control: (a) grid voltages; (b) grid currents; and (c) dc-link voltage under an SLG-voltage sag at MV side of the transformer.

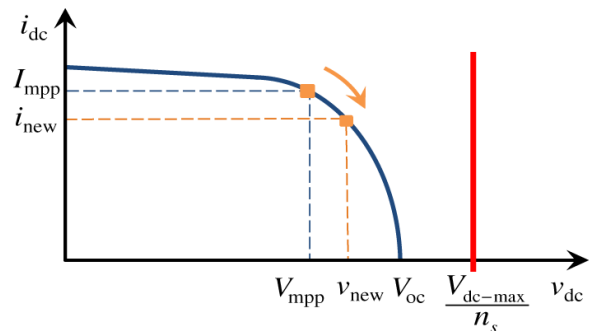


Fig 6. Change in the PV operating point under voltage sag and maximum acceptable dc-link voltage.

It should be mentioned that all the voltage sag case studies in this paper are applied to the MV side for the time period $t = 0.1$ s tot = 0.3 s, whereas the resultant ac voltages and currents shown in the figures are presented with their equivalent magnitudes at the LV side. Fig. 5 shows the generated currents after applying the current limiter in this example. One can observe in Fig. 5(b) that the grid currents are balanced. This is because the active current reference (i_{dref}) is limited to an almost constant value during the voltage sag. It should be mentioned that when operating with low solar radiation and/or small voltage sags, the active current reference may not be limited and therefore, it goes through the current limiter without being affected, i.e., $i_{dref} = i_{dref}$. As a consequence, if the voltage sag was unbalanced, the active current reference and consequently the output currents would contain some low-frequency harmonics.

C. Excessive DC-Link Voltage:

If the active current reference is limited, i.e., $i_{dref} < i_{dref}$, the generated power from the PVs is more than the injected power into the electrical grid. As a consequence, some energy is initially accumulated into the dc-link capacitor, increasing the dc bus voltage as shown in Fig. 5(c). In a single-stage GCPPP, as the dc-link voltage increases, the operating point on the I-V curve of PV array moves toward the open-circuit voltage point (V_{oc}), which leads the PV current to decrease, as shown in Fig. 6. The power generated by the PV panels

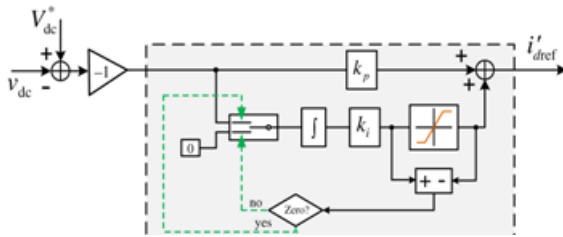


Fig 7. PI controller with an anti-wind-up technique.

Is reduced because the operating point is taken away from the maximum power point (MPP) and therefore, less active current is injected into the ac side. This happens until the GCPPP reaches a new steady state where the dc-link voltage stops increasing. Thus, single-stage GCPPPs are self-protected because the generated power is reduced when the dc-link voltage increases under ac faults. It should be mentioned that the inverter has to withstand the worst case of the dc-link voltage, which is produced when the voltage provided by the PV modules reaches the open-circuit value (Voc) under the maximum solar radiation expected on the generation site. Hence, the number of PV modules connected in series (ns) has to be limited in the design of the GCPPPs so that the dc-link voltage is never higher than the maximum acceptable value of the inverter (Vdc-max).

$$n_s \leq \frac{V_{dc-max}}{V_{oc}}$$

Fig. 6 shows this concept in the case of a single-stage GCPPP. A problem that may appear because of the deviation of the MPP during the voltage sag is that, after the fault being cleared, the dc-link voltage and ac currents may take along time to reach the pre-fault values, as shown in Fig. 5(b) and (c). The reason is that the error in the dc-link voltage produces accumulation of control action to the integral part of the proportional-integral (PI) controller (Fig.4). This control action is limited by the current limiter and thus it has no effect on the grid currents. However, when the voltage sag ends, the excessive control action accumulated in the integral part of the controller has to be compensated by an input error in the opposite direction.

As a consequence, the dc-link voltage is reduced below the reference value. In this case, a significant decrease of the dc-link voltage may lead to inverter losing control and be disconnected. To overcome this issue, an anti-wind-up technique is applied to stop the PI controller accumulating excessive control action when it exceeds a specified value [30]. The schematic of the anti-wind-up technique is shown in Fig. 7 in which V^*_{dc} and v_{dc} are the reference and actual dc-link voltages, respectively. The improved results when applying the anti-wind-up technique are depicted in Fig. 8. In this case, once the grid fault is cleared, the dclink voltage recovers to the pre-fault value with no perceptible overcompensation.

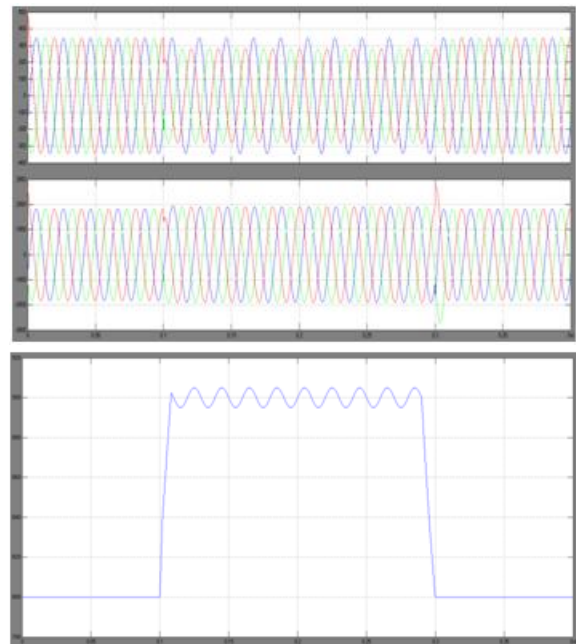


Fig 8. Application of an anti-wind-up technique to the PI controller: (a) grid voltages; (b) grid currents; and (c) dc-link voltage under 60% SLG voltage sag at MV side of the transformer.

IV. GRID FAULTS

CLASSIFICATION OF GRIDFAULTS IN GCPPP SYSTEM:

Faults in PV system can be identified in two side of the system: DC side and AC side, the interface between this to part is DC/AC inverter that connected to grid. The classification of faults is shown in Figure 9.

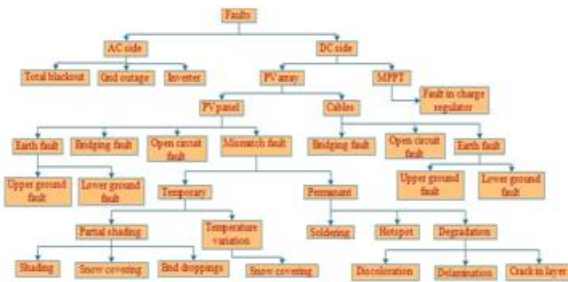


Fig .9. Classification of GCPP faults

A) Faults in DC side:

The faults occur in DC side of the GCPV system is classified into two major types: Fault in PV array and Fault in MPPT

B) Faults in PV Array:

Faults in PV arrays involve two main groups, PV panel fault and cabling. The most common types of fault in PV Panel/Module are Earth Fault, Bridge Fault, Open Circuit Fault and Mismatch Fault.

C) PV PANEL / MODULE FAULT

a)Earth Fault:

Earth of grounding shall be provided for PV system such as system grounding and equipment grounding. In system grounding, the negative conductor is grounded through the earth fault protection device (gfpd) in the pv inverter. The exposed non-current-carrying metal parts of pv module frames, electrical equipment, and conductor enclosures should be grounded in equipment grounding. two types of earth faults namely lower earth fault and upper earth fault can occur. in lower earth fault, the potential fault point is upper than half of the maximum voltage power point. And the upper earth fault will create large backed current and very high earth-fault current. Without any sensor, these faults are identified, when the sign of the monitored primary current of the solar inverter is changed. When the primary current becomes negative, the solar inverters initiate a controlled internal short circuit.

b) Bridging fault:

When low- resistance connection recognized between two points of different potential in string of module or cabling, the bridging fault will occur. Insulation failure of cables such as an animal chewing through cable insulation, mechanical damage, water ingress or corrosion causes these faults.

c) Open Circuit Fault:

An open circuit fault occurs, when one of the current-carrying paths in series with the load is broken or opened. The poor connections between cells, plugging and unplugging connectors at junction boxes, or breaks in wires cause these fault.

d) Mismatch Fault:

When the electrical parameters of one or group of cell are changed from other, the mismatches in PV modules will occur. These fault results in irreversible damage on PV modules and large power loss. These faults can be classified into permanent and temporary mismatches. Temporary mismatches occurs when a part of the panels array are shaded by shade from the building itself, light posts, chimneys, trees, clouds, dirt, snow and other light- blocking obstacles . Non-uniform temperature can identified due to snow covering. Permanent mismatch occurs due to faults in hotspot, soldering and degradation. Hot spot heating happens when the operating current exceeds the reduced short circuit current of a shadowed or faulty cell or group of cells within the module. Soldering fault can be identified in resistive solder bond between cell and contacted ribbons. Discoloration, de lamination and transparent layer crack result in degradation fault.

e) Fault in cables:

Bridging Fault, Open-Circuit fault and Earth Fault are occur in power line carrier and cabling system. An aged connection box at the back side of a solar panel or in the corner and bend aria of cable cause bridging fault. Upper earth and lower earth faults occur between panels and ground.

It results in dropped output voltage and power, and can be dangerous if the leakage currents are running through a person.

D) MPPT Fault:

MPPT increases the power fed to the inverter from PV array. The performance of MPPT degrades when the failure occurs in the charge regulators. The output voltage and the output power reduces when fault occur in MPPT.

E) FAULTS IN AC SIDE:

In AC side two types of faults can be identified: total black out which measured as exterior fault for system, lighting and unbalanced voltage or grid outage for AC part defect such as weaker switch, over current or over voltage and etc. Meanwhile most PV inverters having transformers that could give good galvanic isolation between PV arrays and utility grids and perfect electrical protections. The AC output power will become low and DC output power remains the same, when there is a fault in the inverter.

V. BATTERY ENERGY STORAGE SYSTEM:

The battery energy storage system (BESS) that was integrated into the PV array in the model was based on a number of different industry projects that are either operational or under construction. The general setup of the BESS as it is designed in this model is that it would be connected to the grid at a common bus with a PV project. There are other ways to integrate these energy storage systems into the grid, but this is one of the most common for its ease of control, and re-configurability. It is also common because it yields itself well to situations where utilities would want to construct a system at the substation for regional energy storage, as well as situations where a particular project manager would like to build a system at the substation to mitigate the variability of their privately held PV array nearby. The latter of these situations is the variety that much of this thesis is based on, and regardless of the owner of the PV array, many BESSs are setup based specifically on the parameters of a

nearby solar site in terms of the anticipated required capacity and discharge capabilities.

A) Core Energy Storage Attributes:

The goal of this thesis has been to distill a variety of different technologies down to several core attributes, and to model these attributes in such a way that could be adjusted dynamically to observe the performance of the system under certain configurations. In order to observe the affect of the battery type on the performance of the system, the fundamental attributes of the battery type were determined to be

- Peak charge/discharge rate
- Energy capacity
- Maximum depth of discharge
- Capacity factor
- charge/discharge efficiency

B) BATTERY TYPE:

The battery type is of the utmost importance in terms of the possible range of the parameters of the BESS. Some of the technical specifications of the battery types were not used explicitly in the model, but rather implicitly. The technical specifications for some battery types commonly used in grid-level storage are outlined in this section, as well as some less-commonly used ones-to give the reader a sense of perspective and why some qualities are preferred over others when choosing a battery configuration for a particular system. For each of these types, the relevant model parameter range is given and related to the chemical or physical makeup of the battery type.

a)Lead-Acid (Pb-Acid)

Batteries are known for their high power to weight ratio from high maximum current throughput, but are hampered by their low overall energy to weight ratios. It is for this reason that their primary application has been in traditional internal combustion automobiles as a method to supply power to the lighting and ignition systems. They are not typically found in consumer electronics or electric vehicle applications because of this low energy to weight ratio.

In applications where weight and size are unimportant, such as grid-level energy storage, they are more common. Still, they are often overshadowed in grid storage applications by other battery types such as NiCd and NiMH that offer substantially greater capabilities in terms of energy and power density, and average cycle life albeit at a higher cost.

b) Nickel-cadmium (NiCd)

Batteries have similar applications to those of NiMH batteries. They have the disadvantage of being produced using the highly toxic metal cadmium. However until recently they were cheaper to produce than other similar batteries. The lowering cost of production of NiMH batteries has led to stricter regulation on NiCd batteries for consumer use, though their use in specialized application remains popular because of their ability to tolerate high discharge rates with no loss of capacity or damage to the battery cells. They can also be discharged much deeper and for more prolonged periods of time than other batteries.

c) NiCd Batteries

Have a charge cycle energy efficiency of between 60% and 90%. The upper extent of which places them ahead of almost every other battery type. They have an energy density of 40-60 Wh/kg, and a power density of 140-180 W/kg. The self discharge rate is low, at about 1% per day, though this would not likely be relevant in a BESS system connected at a common bus with a PV array. In this setup, the battery would likely cycle once every 1-2 days. One of the more relevant aspects of NiCd batteries, however, is their cycle life which averages approximately 3000 charge cycles. This would be a major component of the lifetime cost of a BESS that selected this particular battery chemistry. NiCd batteries are some of the most commonly used battery types in grid-scale energy storage.

d) Nickel-metal hydride (NiMH)

Batteries have two to three times the energy density of nickel-cadmium batteries – though less than that of lithium-ion. Their main disadvantage is a higher rate of self-discharge relative to other battery chemistries.

They can discharge safely from 1.4V/cell at full charge to a maximum discharge of just over 1V/cell, with an average 1.25V/cell during discharge, (under a current load of 0.5 A). This delivers a more constant voltage over the entire charge cycle than other battery types, though over-discharging can damage the cells by polarity reversal. NiMH batteries are well suited for high current drain applications because of their low internal resistance. They are often used in digital cameras, as well as electric automobiles. NiMH batteries are well suited for many applications where high power-to-weight ratio is a priority. They are typically not chosen for grid-level storage because there is rarely an impetus to find a smaller, lighter battery only one that stores enormous amounts of energy efficiently. Unfortunately, overall charge cycle efficiency is not a strong suit of a typical NiMH battery, with documented rates of between 50-80%. Furthermore, their self-discharge rate without separator devices is considered relatively high. They have a working life of between 500 and 2000 cycles, depending on application. Because of these reasons, they have not been included in the model.

e) Lithium-ion (Li-ion) batteries

Have good energy efficiency rates of 85-95%, and of course have excellent energy density and power density ratings of 100-200 Wh/kg and 360 W/kg, respectively. It is these characteristics that enable them to be the dominant form of energy storage in consumer electronics, where small size and weight are paramount. They have a relatively low self-discharge rate between 5% and 10% per month, depending on the specific type of Li-ion battery chemistry, and their working lifetime consists of approximately 3000 charge cycles in line with previously mentioned battery types. Their cost is prohibitively high for most applications in grid-level energy storage, where larger, cheaper alternative abound. The cost of lithium based batteries is expected to continue to rise as they are used more frequently in consumer electronics and electric vehicle applications, while the world's known supply of lithium is being depleted faster than new stores are discovered.

However, at the AES Laurel Mountain project in West Virginia, 32 MW of Li-Ion batteries provide reserve capacity for a 97 MW wind farm. The installation costs of the BESS are said to have been \$900 per kW, bringing the total installation cost to \$28.8 million.

f) Vanadium flow batteries

Offer somewhat greater simplicity because of their use of only one electrolyte solution, rather than two as is the case with most other flow batteries. They can be discharged completely without damaging the system components, and their stated cycle life is greater than 10,000 cycles. Their overall cycle efficiency, however, ranges from 65% to 72%, depending on the manufacturer (70% is the value used in the model). This contributes to an approximate overall lifetime cost of \$915 per kWh. Vanadium flow batteries have a low energy-to-volume ratio, though this is less of a concern with grid-level energy storage applications. Additionally, though they constitute less complex systems than other flow batteries, they still require more complex systems than most other traditional batteries, and thus introduce more points of potential failure and required maintenance.

Type	Min. Charge (%)	Efficiency (%)	Cycles	Cost (\$/kWh)
Pb-Acid	30	75	1500	135
Ni-Cd	0	75	3000	540
Na-S	0/15	89	2500/4500	500
Li-Ion	20	93	3000	1145
Vanadium	0	70	10000	915

Table 2. Battery types included in the model, and their attributes, ordered approximately by their date of first demonstration

C) BESS COMPONENT OF MODEL:

In designing the BESS component of the model, I was determining the parameters that would most actively be manipulated to analyze the possible configurations of the energy storage at the PV site. In setting up the parameters, I looked at what values were available to project managers to change during the design phase of the system, (such as the charge and discharge speed, which are related to battery chemistry), as well as the parameters that would be adjusted from month-to-month, week-to-week or day-to-day by the facility operator or utility coordinator.

These parameters included the application that was being utilized by the system, and according to which application was being used the parameters would include items such as the steady-state charge level, the output leveling target, or a parameter such as the point of transition from off-peak to on-peak power for time-shifting purposes. The ramp rate was of course a primary constraint for each application, and when looking at what the ramp rate of the BESS should be, I looked at what the goal of a system operator would be in terms of how long the PV plant gave the utility to adjust other reserves when the plant came online in the morning or reduced its output in the evening. I felt that a good goal would be to reduce the need to utilize spinning reserves, if not the need to maintain reserves altogether. Spinning reserves are a source of wasted energy in that for a plant to be considered to have spinning reserves it must essentially “idle” with no power output so that if needed, it can ramp up in response to variability’s such as those from solar and wind power over the course of just a few minutes. The ability of any one plant to ramp up in response to variability is finite, with the best current natural gas plants only able to ramp up 63 MW within a minute. We will not be able to completely eliminate the need for reserve capacity on the grid until we are able to store enough wind and solar energy to reliably power the grid 24/7. Non-spinning reserves generally require approximately 30 minutes to “spin-up” from their initial position, and so I felt that this 30 minute window would be a good goal for the model to achieve. Therefore, the ramp-rate constraint was defined to be not more than the nameplate power capacity of the PV facility over 30 minutes. Depending on the application, not all second-to-second variation that exceeded this would be eliminated. For example, in the Absolute Leveling application, the only ramp rates over the course of the day would be the initial ramp-up from zero to steady-state output, and the final ramp-down from the steady-state output back to zero. Both of these ramping periods would be constrained to last at least 30 minutes. However, for other applications, such as Reactive Leveling, some intermittent variability throughout the day that might

be at a higher rate than 100%/30 minutes would be allowed because of the caveat that variability within a certain threshold would be allowed, such as that within 10% of the peak output. In order to set both the ramp up and ramp down times to the minimum ramp period, the model had to first calculate the maximum projected output for that particular day.

VI. DESIGN AND ANALYSIS OF SINGLE STAGE CONVERSION WITH BATTERY CONVERTER:

Among various renewable energy resources, PV and wind power are most rapidly growing renewable energy sources. The PV source is a nonlinear energy source and direct connection of load will not give optimum utilization of the PV system. In order to utilize the PV source optimally, it is necessary to provide an intermediate electronic controller in between source and load under all operating conditions. Using this electronic controller it is possible to operate the PV source at maximum power point (MPP), thus improving the energy efficiency of the PV system. Many control algorithms have been reported in the literature to track maximum power from the PV arrays, such as incremental conductance (INC), constant voltage (CV), and perturbation and observation (P&O). The two algorithms often used to achieve maximum power point tracking are the P&O and INC methods. Many DC-DC converter topologies are available to track the MOP imp generating system. Cascade connection of conventional converters provides wider conversion ratios. One of the major advantages of these converters is a high gain and low current ripple. However, this configuration has a drawback that the total efficiency may become low if the numbers of stages are high, owing to power losses in the switching device. A quadratic converter configuration is also available that uses single switch and achieves quadratic gain. An interesting attractive converter topology is high gain integrated cascaded boost converter having n-converters connected in cascade using a single active switch. The instability caused by the cascade structure is avoided, when compared with the conventional cascade boost

converter. This class of converters can be used only when the required number of stages is not very large, else the efficiency will be reduced. However, this class of converters for PV applications are not reported in the technical literature. Micro-grid power converters can be classified into (I) grid-feeding, (ii) grid-supporting, and (iii) grid-forming power converters. There are many control schemes reported in the literature such as asynchronous reference theory, power balance theory, and direct current vector control, for control of μ G-VSC in micro grid application. These algorithms require complex coordinate transformations, which is cumbersome. Compared to the control strategies mentioned above, the Instantaneous symmetrical component based control proposed in this paper for micro-grid applications is simple in formulation, avoids interpretation of instantaneous reactive power and needs no complex transformations.

A) SYSTEM DESCRIPTION:

The envisaged system consists of a PV/Battery hybrid system with the main grid connecting to non-linear and unbalanced loads at the PCC as shown in the Fig. 1. The photovoltaic system is modeled as nonlinear voltage sources. The PV array disconnected to HICK dc-dc converter and bidirectional battery converter are shown in Fig. 1, which are coupled at the dc side of a μ G-VSC. The HGICB dc-dc converter is connected to the PV array works as MOPPET controller and battery converter is used to regulate the power flow between dc and ac side of the system.

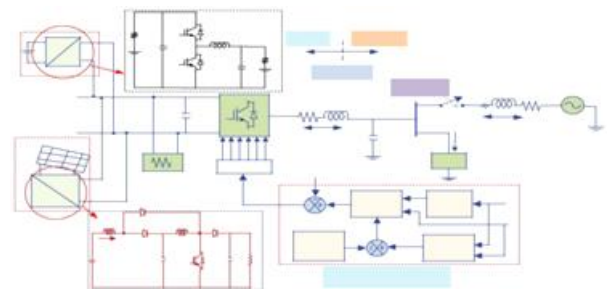


Fig 10. Hybrid Energy Conversion System under consideration

The proposed control strategies for PV hybrid generating systemic developed and simulated using Mat lab/SEMOLINA under different solar insulation levels. In order to capture the transient response of the proposed control system, PV insulation is assumed to increase from 200 to 1000 /m²at 0.3 s, and decreases from 1000 to 200 W/m²at 0.5 s. This abrupt increase or decrease is assumed in this work in order to test the robustness of the proposed control algorithm. As a result, the inductor current of the HICK converters varied to track the maximum power accordingly and the power flow between the μ G-VSC, grid and load is also varied under above the operating conditions.

B)MPPT Tracking Performance of HGICB Converter:

The dynamic performance of HGICB converter with P&O MPPT algorithm at two different insulation levels is shown in Fig. 5. Variable PV voltage and current in proportion to insulation levels are applied to HICK converter and as a result, the duty cycle is calculated using the MOPPET algorithm. The PV characteristics at two insulation levels are shown in Fig. 5(a)-(b). From Fig. 5 (a), the maximum power, current and voltage are 2.6 kW, 14 A and 190 V respectively and these values are tracked by HICK converter which are shown in Fig. 5 (d)-(f). Tracked values of PV power, voltage and currents are given in Table II for the above operating insulation levels. From these results it can be concluded that, HICK converters tracking maximum power closely at all operating conditions.

C)Performance of μ G-VSC with different insulation levels:

The μ G-VSC is actively controlled to inject the generated active power as well as to compensate the harmonic and reactive power demanded by the unbalanced and non-linear load at PAC, such that the current drawn from grid is purely sinusoidal at UP. The dynamic compensation performance of μ GVSC using proposed control algorithm with insulation change adnoun linear unbalanced load currents are shown in the Fig.7.1 (a)-(d)along with grid side

currents. When insulation $G = 200 \text{ W/m}^2$, the maximum power extracted from PV arrays is 2.5 kW and the total cloud power (4.5 kW) is partly supplied by PV arrays and the remaining dc load power (2 kW) is drawn from grid through the bidirectional μ G-VSC. Here observed that the power flows from ac side to dc link as shown in the Fig.7.1 When insulation $G = 1000\text{W/m}^2$, the maximum power available from PV arrays is 12.5 kW, part of this power (4.5 kW) is supplied to dc load and remaining power (8 kW) is supplied to the ac load through bidirectional μ GVSC. In this case, the power flows from dc link to ac side. This shows the bidirectional power flow capability of μ G-VSC. These dynamics of power flows can be seen from Fig.7. The corresponding variations in the grid current against grid voltage with UPF are showing the along with dc link voltage variations.

VII. MATLAB/SIMULATION RESULTS MATLAB/SIMULATION INTRODUCTION

MATLAB is a high performance language for technical computing. It integrates computation, visualization and programming is an easy to use environment where problems and solutions are expressed in familiar mathematics notation. Typically uses include.

- Math and computation
- Algorithm development
- Data acquisition
- Modelling, simulation and Prototyping
- Data analysis , exploration and visualization
- Scientific and engineering graphics

MATLAB is an interactive system whose basic data element is an array that does not require dimensioning. This allows solve in many technical computing problem especially those with matrix and vector formulations, in a fraction of the time it would take to write a program in scalar non-interactive language such as C or FORTRAN.

The matlab system consist of six main parts:

- a) Development environment
- b) The MATLAB mathematical function library

- c) The MATLAB language
- d) Graphics
- e) The MATLAB application program interface(API)
- f) MATLAB documentation

MATLAB/SIMULATION RESULTS:

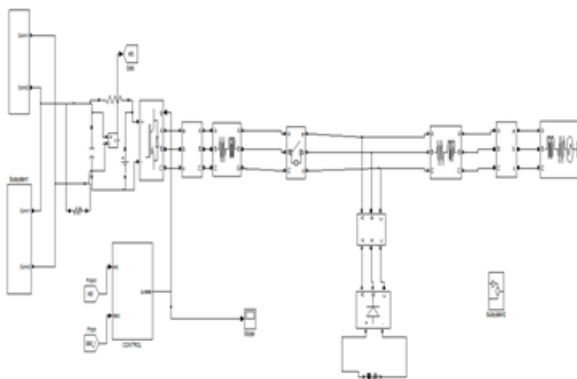


Fig 11. proposed single stage converter with battery

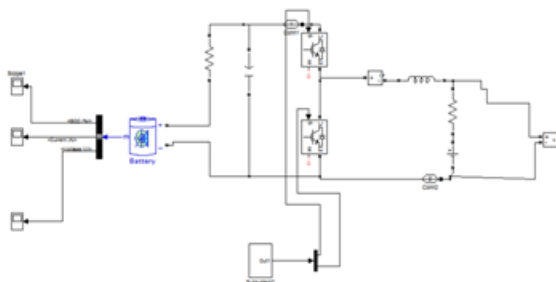


Fig 12. Battery converter model

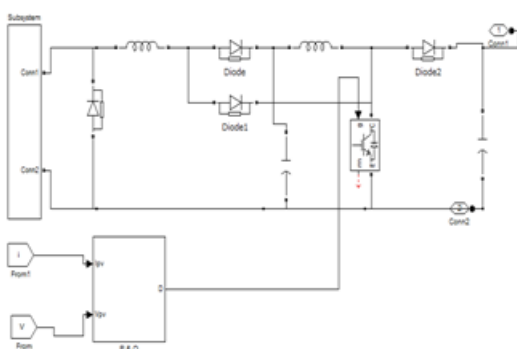


Fig 13. PV array model with boost converter



Fig 14. Irradiance

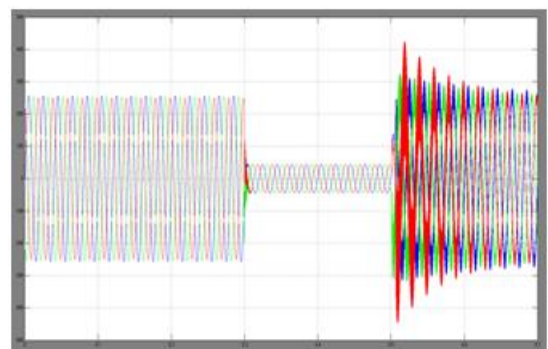


Fig 15. Simulation results using proposed control approach for Micro-grid side voltage

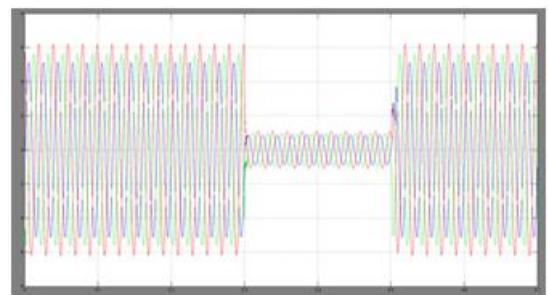


Fig 16. Simulation results using proposed control approach for Micro-grid side current

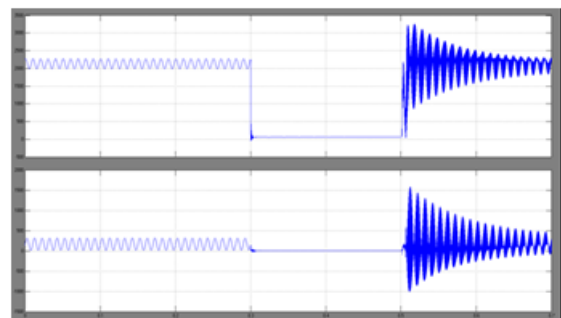


Fig 17. Active power and reactive power

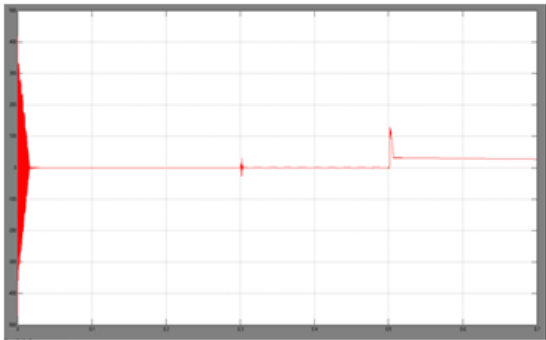


Fig 18. Inverter Voltage

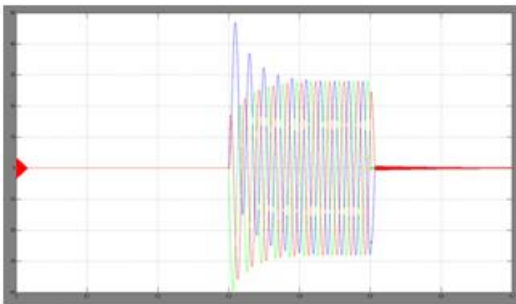


Fig 19. Inverter Currents

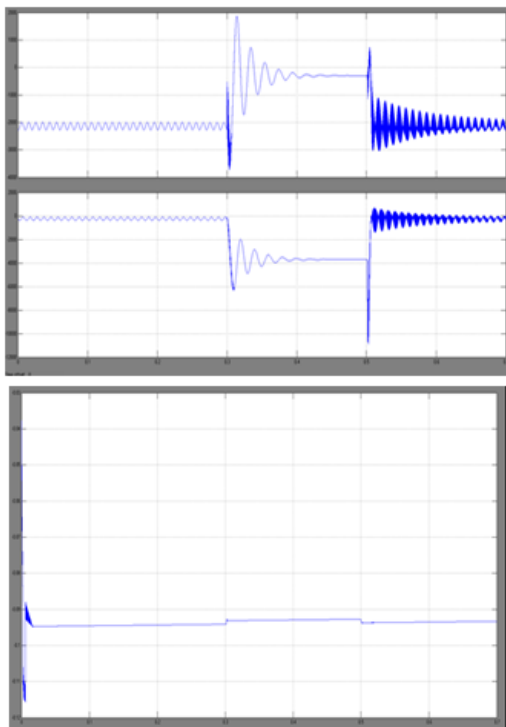


Fig 20. Simulation results: performance of proposed control approach (a) Grid Voltages and currents (b) Dc Link Voltage Dynamics with different Isolations.

VIII. FUTURE SCOPE:

The model of the hybrid PV-diesel generator-battery plant, which is built in Power Factory, can be used as a base for further analysis with dispatch control. A model of dispatch control must be integrated in order to be able to run a one year simulation if the required input data is available. A one year simulation is useful to study the effects of different dispatch strategies on the operation and cost of the plant. Moreover, the simulation results of one year can be used for more accurate analysis of the fuel consumption of the plant and the lifetime of the battery bank. In addition, it can provide a better economical evaluation compared to one day simulation. Based on one year simulation results, an economical comparison between the control strategies according to the different fuel consumption and different expected lifetime of the batteries can be performed. Battery banks are susceptible to performance degradation according to the aging effect.

The capacity and the DC voltage of the battery decrease by the time, which can negatively affect the performance of the BESS. However, in this thesis; it is assumed that the capacity and the voltage are not affected by the age; because the simulation is only for one day. For a longer simulation, integrating the model of the BESS with the effect of aging can provide more accurate results, which can be used for better analysis of the lifetime and optimum sizing of battery banks. As an important implementation of renewable energy technology in the MENA region, the hybrid PV-diesel generator-battery plant in stand-alone operation can be proposed for Arwad. Arwad is a Syrian island that greatly depends on energy supply from the Syrian main land. However, an implementation of the hybrid plant can improve the performance of energy supply in the island and also improve the socio-economic conditions of Arwad people. The Island has a population of 10,000 inhabitants with an area of 200,000 [m²]. The island is located in the Mediterranean Sea, 3 [km] to the west of Tartus city in the Syrian mainland. As an attractive natural and historical site, implementing renewable energy technology in the island can be a desired option that

helps to preserve the environment. In addition, a PV field is visually more acceptable compared to wind turbines. Furthermore, the diesel generators can be fueled by biodiesel as an additional option of utilizing renewable energy. As a recommendation for future work, the implementation of the analyzed hybrid plant can be studied including the sizing, energy yield and economical evaluation of the plant in Arwa. In fact, a more detailed study case of the implementation of the plant in Syria was planned, but unfortunately the conditions were not suitable for field trips.

APPLICATIONS:

The only one application of this project is in the “MICRO-GRID”

ADVANTAGES:

- 1..The power quality can be improved.
- 2.Mitigation of current harmonics.
- 3.Reactive power can be compensated.

IX.CONCLUSION:

Performance requirements of GCPPPs under fault conditions for single- and two-stage grid-connected inverters have been addressed in this paper. Some modifications have been proposed for controllers to make the GCPPP ride-through compatible to any type of faults according to the GCs. These modifications include applying current limiters and controlling the dc-link voltage by different methods. It is concluded that for the single-stage configuration, the dc-link voltage is naturally limited and therefore, the GCPPP is self-protected, whereas in the two-stage configuration it is not. Three methods have been proposed for the two-stage configuration to make the GCPPP able to withstand any type of faults according to the GCs without being disconnected. The first two methods are based on not generating any power from the PV arrays during the voltage sags, whereas the third method changes the power point of the PV arrays to inject less power into the grid compared with the pre-fault condition. The validity of all the proposed methods to ride-through voltage sags has been demonstrated by multiple case studies performed by

simulations. In these we are using battery energy storage system (BESS) to storage the energy getting from GCPPP system.

REFERENCES:

- [1] M. Mirhosseini, J. Pou, and V. G. Agelidis, “Single-stage inverter-based grid-connected photovoltaic power plant with ride-through capability over different types of grid faults,” in Proc. Annu. Conf. IEEE Ind. Electron. Soc. (IECON), Nov. 2013, pp. 8008–8013.
- [2] A. Marinopoulos et al., “Grid integration aspects of large solar PV installations: LVRT capability and reactive power/voltage support requirements,” in Proc. IEEE Trondheim Power Tech, Jun. 2011, pp. 1–8.
- [3] G. Islam, A. Al-Durra, S. M. Muyeen, and J. Tamura, “Low voltage ride through capability enhancement of grid connected large scale photovoltaic system,” in Proc. 37th Annu. Conf. IEEE Ind. Electron. Soc. (IECON), Nov. 2011, pp. 884–889.
- [4] P. Dash and M. Kazerani, “Dynamic modeling and performance analysis of a grid-connected current-source inverter-based photovoltaic system,” IEEE Trans. Sustain. Energy, vol. 2, no. 4, pp. 443–450, Oct. 2011.
- [5] A. Yazdani et al., “Modeling guidelines and a benchmark for power system simulation studies of three-phase single-stage photovoltaic systems,” IEEE Trans. Power Del., vol. 26, no. 2, pp. 1247–1264, Apr. 2011.
- [6] A. Radwan and Y.-R. Mohamed, “Analysis and active suppression of ac and dc-side instabilities in grid-connected current-source converter-based photovoltaic system,” IEEE Trans. Sustain. Energy, vol. 4, no. 3, pp. 630–642, Jul. 2013.
- [7] J. Miret, M. Castilla, A. Camacho, L. Garcia de Vicuna, and J. Matas, “Control scheme for photovoltaic three-phase inverters to minimize peak currents during unbalanced grid-voltage sags,” IEEE

Trans. Power Electron., vol. 27, no. 10, pp. 4262–4271, Oct. 2012.

[8] M. Mirhosseini, J. Pou, B. Karanayil, and V. G. Agelidis, “Positive- and negative-sequence control of grid-connected photovoltaic systems under unbalanced voltage conditions,” in Proc. Australasian Univ. Power Eng. Conf. (AUPEC), Sep. 2013, pp. 1–6.

[9] D. Campos-Gaona, E. Moreno-Goytia, and O. Anaya-Lara, “Fault ride-through improvement of DFIG-WT by integrating a two-degrees-of-freedom internal model control, in “Proc. IEEE Trans. Ind. Electron., vol. 60, no. 3, pp. 1133–1145, Mar. 2013.

[10] G. Pannell, B. Zahawi, D. Atkinson, and P. Missailidis, “Evaluation of the performance of a dc-link brake chopper as a DFIG low-voltage fault-ride-through device,” IEEE Trans. Energy Converts., vol. 28, no. 3, pp. 535–542, Sep. 2013.

[11] C. Feltes, H. Wrede, F. Koch, and I. Erlich, “Enhanced fault ride-through method for wind farms connected to the grid through VSC-based HVDC transmission,” IEEE Trans. Power Syst., vol. 24, no. 3, pp. 1537–1546, Aug. 2009.

[12] M. Mirhosseini, J. Pou, and V. G. Agelidis, “Current improvement of a grid-connected photovoltaic system under unbalanced voltage conditions,” in Proc. IEEE ECCE Asia Downunder (ECCE Asia), Jun. 2013, pp. 66–72.

[13] E. Troester, “New german grid codes for connecting PV systems to the medium voltage power grid,” in Proc. 2nd Int. Workshop Conc. Photovoltaic Power Plants Opt. Des. Product., Grid Connect., Mar. 2009, pp. 1–4.

[14] M. Mirhosseini and V. G. Agelidis, “Performance of large-scale grid-connected photovoltaic system under various fault conditions,” in Proc. IEEE Int. Conf. Ind. Technol. (ICIT), Feb. 2013, pp. 1775–1780.

[15] M. Mirhosseini, J. Pou, and V. G. Agelidis, “Single-stage inverter-based grid-connected photovoltaic power plant with ride-through capability over different types of grid faults,” in Proc. Annu. Conf. IEEE Ind. Electron. Soc. (IECON), Nov. 2013, pp. 8008–8013.